AQUA
Water Infrastructure, Ecosystems and Society



IWA PUBLISHING

 AQUA — Water Infrastructure, Ecosystems and Society Vol 72 No 2, 123 doi: 10.2166/aqua.2022.125

# Kinetic and isotherm studies on the removal of reactive Red 2 from aqueous solutions using phosphoric acid activated carbon

Arezoo Mahmoudi[a,b], Seyyed Alireza Mousavi[a,b,*] and Sheida Atashkar[a,b]

[a] Department of Environmental Health Engineering, School of Public Health, Kermanshah University of Medical Sciences, Kermanshah, Iran
[b] Student Research Committee, Kermanshah University of Medical Sciences, Kermanshah, Iran
*Corresponding author. E-mail: seyyedarm@yahoo.com; sar.mousavi@kums.ac.ir

## ABSTRACT

In the current study, an alternative precursor for the production of activated carbon (AC) is introduced using grape wood. The AC structures and functional groups were studied using a scanning electron microscope (SEM) and Fourier transform infrared spectroscopy (FTIR). The efficiency of prepared AC has been investigated in the removal of Reactive Red 2 (RR2) from an aqueous solution. The effect of main variables, namely dye concentration (100–500 mg $L^{-1}$), contact time (10–90 min), adsorbent dosage (0.25–12.25 g $L^{-1}$), and initial pH (3–11) have been assessed on the adsorption process in order to find out the optimum conditions. Langmuir, Freundlich, and Temkin adsorption isotherm models were applied to describe the characteristics of adsorption behavior. Kinetic data were fitted to pseudo-first-order, pseudo-second-order, and intra-particle diffusion models. Based on the results, the highest removal efficiency (97.96%) of RR2 dye was obtained at an initial concentration of 100 mg $L^{-1}$, adsorbent dose of 12.25 g, contact time of 90 min, and pH 3, which indicated a significant sorption efficiency. The rate of the adsorption fitted well to a pseudo-second-order kinetic model ($R^2 = 0.99$). In addition, the Temkin adsorption isotherm model was found to fit the experimental data ($R^2 = 0.99$).

**Key words:** activated carbon, adsorption, central composite design, optimization, reactive dye

## HIGHLIGHTS

- To investigate the Reactive Red 2 adsorption using activated carbon from grape wood wastes.
- To study the effects of independent variables on the Reactive Red 2 removal using activated carbon.

## GRAPHICAL ABSTRACT

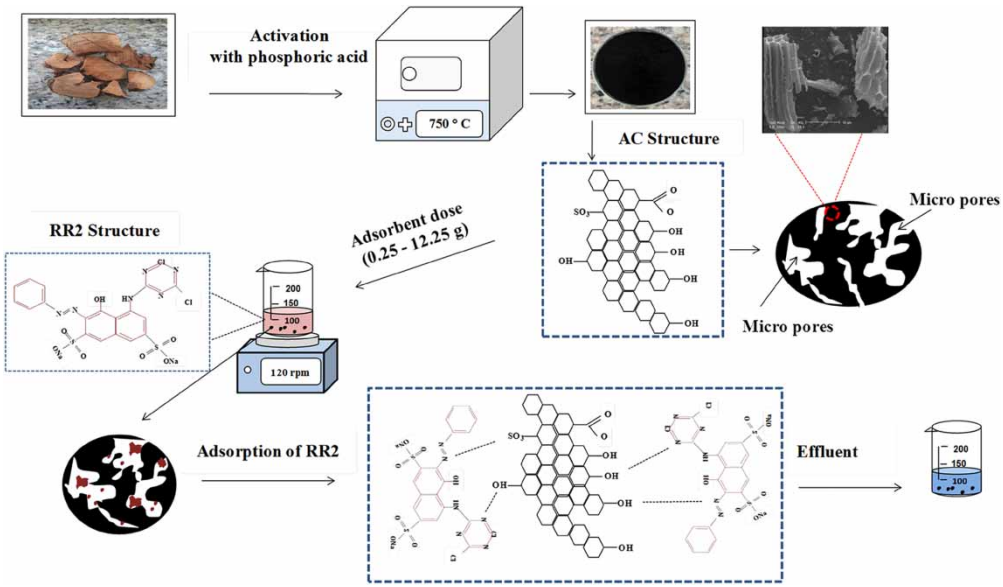

## ABBREVIATIONS

| | |
|---|---|
| RSM | response surface methodology |
| CCD | central composite design |
| $C_0$ | initial concentration of dye solution (mg $L^{-1}$) |
| $q_m$ | maximum adsorption capacity reflected a complete monolayer (mg $g^{-1}$) in Langmuir isotherm model |
| $C_e$ | dye concentration (mg $L^{-1}$) at equilibrium |
| $V$ | volume of solution (L) |
| $W$ | weight of adsorbent (g) |
| $q_e$ | equilibrium adsorption capacity (mg g) |
| $k_2$ | the rate constant of pseudo-second-order adsorption (g $mg^{-1}$ $min^{-1}$) |
| $\beta_0$ | offset term |
| $K_F$ | isotherm constant indicates the capacity parameter (mg $g^{-1}$) related to the intensity of the adsorption |
| $\beta_{ii}$ | squared effect |
| FTIR | Fourier transform infrared spectroscopy |
| NaOH | sodium hydroxide |
| $\beta_{ij}$ | interaction effect |
| $R^2$ | correlation coefficient |
| $\%R$ | percentage of adsorption process efficiency |
| $b$ | Langmuir constant or adsorption equilibrium constant (L $mg^{-1}$) that is related to the apparent energy of sorption |
| $Y$ | predicted response |
| $n$ | Freundlich constant |
| AC | activated carbon |
| RR2 | Reactive Red 2 |
| $k_1$ | the equilibrium rate constant of pseudo-first-order adsorption (g $g^{-1}$ $min^{-1}$) |
| $\beta_i$ | linear effect |
| $K_L$ | Langmuir constant or adsorption equilibrium constant (L $mg^{-1}$) that is related to the apparent energy of sorption |
| SEM | scanning electron microscope |
| $H_3PO_4$ | phosphoric acid |
| $H_2SO_4$ | sulfuric acid |

## INTRODUCTION

Activated carbon (AC) or activated charcoal is a common term used to describe carbon-based materials (González-García 2018; Gao *et al.* 2020). In fact, AC is a porous carbonaceous solid material that is produced from carbon-rich raw materials such as coal or biomass through thermal or thermochemical processes (Ukanwa *et al.* 2019). Carbon structures contain the main functional groups such as quinone, phenol, lactone, carbonyl, and carboxyl that are responsible for adsorbing contaminants. Nitrogen, hydrogen, sulfur, and oxygen are also present in the form of functional groups or chemical atoms in the AC structure (Heidarinejad *et al.* 2020; Jha *et al.* 2021). Hydrogen, oxygen, and other heteroatoms in the raw materials or chemicals used in the activation are attached to the ends and corners of the crystal structure to form various functional groups on the AC surface (Demiral *et al.* 2021). Consequently, AC has permanent applications in water treatment and desalination, wastewater treatment, and air purification due to its unique characteristics such as its internal porous structure (consisting of pores having diverse size distribution) and high surface area (Heidarinejad *et al.* 2020). The results of various studies show that AC has a significant effect in removing dyes, solvents, heavy metal ions, pesticides, pharmaceutical and personal care products (PPCPs) as well as organic pollutants from water and wastewater (Wong *et al.* 2018). Among the pollutants, dyes are used in large quantities in various industries such as textiles, leather, cosmetics, paper, printing, plastics, medicine, food, etc (Vishani & Shrivastav 2022). Dyes are toxic and dangerous for aqueous circumstances and live organisms, which are visible and detectable in small amounts (below 1 ppm) and influence the water environment considerably (Cherifi *et al.* 2013). The dyes prevent sunlight penetration into the water, reduce photosynthesis and change the solubility of gases in the water (Ali *et al.* 2017). Dyes can be divided into groups of reactive, acidic, direct, cationic, dispersed, and vat dyes based on their characteristics and application. Among the various dyes, reactive dyes are one of the most commonly used synthetic dyes due to their stability, high solubility, high dye variety, and low price, which are widely used for dyeing cotton and other cellulosic fibers, nylon, and wool (Mousavi *et al.* 2021). Reactive Red 2 (RR2) represents one of the many types of reactive azo dyes shortly named RR2. RR2 dye is a covalent and strongly bonded compound, thus naturally difficult to disintegrate (Mendonça *et al.* 2019). This dye is widely used for dyeing cellulosic fibers in the textile industry. On the other hand, only

60–70% of the reactive dye reacts with the fibers during the dyeing process, and the remainder is hydrolyzed and released into the environment (Maas & Chaudhari 2005).

Currently, the demand for AC is increasing every year, and based on forecasts, the market growth is estimated at 4.6% per year. Also, according to published statistics, the global AC market is worth several billion dollars annually (Ukanwa *et al.* 2019; Lotfy & Roubík 2021). However, due to the high cost of importing AC in developing countries, researchers are trying to make AC from cheap materials. The production of AC from agricultural wastes cause to reduce costs and makes it more environmentally friendly (Selvanathan *et al.* 2015). Therefore, in recent years, there has been a growing interest in the production of ACs from agricultural by-products and residual wastes. Using the produced agriculture by-products as a starting material for the production of AC as an efficient adsorbent adds value to the harvested crops (Jjagwe *et al.* 2021). Agricultural by-products can be generally classified into two groups of hard and soft agricultural by-products. Hard agricultural by-products include hard, dense residues that are not easily compressed, such as wood, apricots, pecan or walnut shells, and the stones of dates, or cherries. Also, the second group includes soft and compressible agricultural by-products with low density, such as peanut shells, rice husk, soybean shells, sugarcane bagasse, etc. (Paraskeva *et al.* 2008). The main components of woody agricultural residues are similar to other lignocellulosic materials, mainly composed of polysaccharides such as 40–50% cellulose, 20–30% hemicellulose, 20–25% lignin, and 1–5% ash which makes them an attractive source for AC production (Lopes & Astruc 2021). In fact, agricultural wastes due to availability, carbonaceous nature, low inorganic content, high volatile matter content, high density, low degradation upon storage, the potential for activation, having microstructures within itself, and producing high yield when activated are the most suitable for producing AC (Lotfy & Roubík 2021; Jjagwe *et al.* 2021). In this regard, in order to reduce the waste of horticultural products, reduce the overall costs of water and sewage treatment (through reducing the import of chemicals) and create income for poor communities, grape wood waste was used to produce active carbon. Therefore, the main goal of this article was to explain the adsorption mechanism through experimental and theoretical studies and as a result to provide new interpretations of the removal of RR2 at the molecular level of the adsorbent. Also, the central composite design (CCD) based on response surface methodology (RSM) was used to obtain a possible correlation with the results of adsorbent characterization, their adsorption properties, and dye adsorption mechanism. Overall, the integrated analysis of experimental and theoretical findings helps to obtain new insights into the adsorption of RR2 dye using AC prepared from grape wood.

## MATERIALS AND METHODS

### Chemicals and reagents

RR2 with 98% purity (Merck Company, Germany) has been used for preparing stoke solution, 1,000 mg $L^{-1}$ of RR2 was dissolved in 1 L of distilled water. The RR2 specification is shown in Table 1 (Hameed & Ismail 2018). The chemical activation of the adsorbent was carried out by using 85% phosphoric acid ($H_3PO_4$). In this experiment, sulfuric acid (98%) and sodium hydroxide (Merck, Germany) were used to adjust the pH. The RR2, sodium hydroxide (NaOH), sulfuric acid ($H_2SO_4$), and phosphoric acid were all analytical grades and used without further purification.

**Table 1** | The characterization of RR2 dye

| Characteristics | Values |
|---|---|
| Molecular formula | $C_{19}H_{10}Cl_2N_6Na_2O_7S_2$ |
| λmax (nm) | 540 |
| Molecular weight (MW) | 615.33 g/mol |
| Chemical structure | 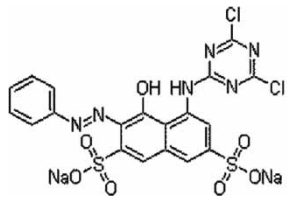 |

### Synthesis of AC

The source of produced AC was the residues of grape wood provided from gardens in the suburbs of Kermanshah, Iran, and then transferred to the laboratory (Figure 1). The raw material was washed using distilled water several times to remove the contamination and impurities. In the next step, the grape wood was cut into smaller pieces. Then, the grape wood was dried in an oven (Memmert 854, Germany) at 100 °C for 3 h. Chemical activation was accomplished with phosphoric acid. Grape wood was submerged for 8 h with a mass ratio of 1:10 with 85% phosphoric acid. Then the mixture of precursor and chemical activator was heated to 100 °C for 24 h. For carbonization, the achieved product was placed in the electric furnace (Nabertherm Company, Germany), at 750 °C for 1 h. After natural cooling of the adsorbent, it was washed with 0.1 mol $L^{-1}$ NaOH, $H_2SO_4$, and distilled water, respectively, until reaching a neutral pH. The prepared sample was then put in a dry glass bottle.

### Physicochemical characterization

Microscopic and chemical properties of prepared AC were studied by scanning electron microscope (SEM) and Fourier transform infrared (FTIR) methods. Microscopic images of AC (adsorbent) were obtained by scanning electron microscope (Jeol JSM 840A, Japan). Fourier transform infrared spectroscopy (FTIR) was used to determine the vibrational frequency changes in the functional groups of the AC. The spectra were collected by FTIR (ShimaDZU IRPrestige, Japan model) within the range of wave number of 400–4,000 $cm^{-1}$.

### Central composite design

A standard RSM design known as CCD was used to study the parameters for the adsorption of RR2 with AC. RSM is a set of statistical and mathematical techniques that uses quantitative data from experiments to determine regression model equations and operating conditions that are useful for developing, improving, and optimizing processes (Karimifard & Moghaddam 2018; Ghaedi *et al.* 2019). The main purpose of RSM is to determine the optimal operating conditions for the system (Jensen 2017). Also, this design includes a bilevel factorial design which has one or more central points in the empirical conditions. Generally, the CCD consists of 2k factorial run with 2k axial runs and $x_0$ number of center points (six replicates). The number of experimental runs was calculated from the following Equation (1):

$$N = 2^f + 2f + N_0 \tag{1}$$

**Figure 1** | Photograph of grape wood residues.

where the quantity of the parameters that are studied is shown by $f$, factorial points are shown by $2^f$, axial points are shown by $2f$ and $N_0$ represents the replicates of center points. The center points are used to determine the experimental error and the reproducibility of the data. The independent variables are coded to the (−1, 1) interval where the low and high levels are coded as −1 and +1, respectively (Table 2). With the software suggested, the experiments were at 78 runs. Each experiment was carried out three times and the average results of the RR2 dye removal evaluation over the AC and their corresponding standard deviation values were reported. Table 3 shows the empirical data which contains the design matrix and responses. The quadratic model based on (Equation (2)) was used to develop a predictor model (Shahbazi *et al*. 2020; Onu *et al*. 2021; Nguyen *et al*. 2022).

$$Y = \beta_0 + \sum_{i=1}^{k} \beta_i X_i + \sum_{i=1}^{k} \beta_{ii} X_i^2 + \sum_{i=1}^{k-1} \sum_{j=2}^{k} \beta_{ij} x_i x_j + e \tag{2}$$

where $j$ represents the quadratic coefficient; $i$ represents the linear coefficient; $x$ represents independent variables; $\beta$ refers to regression coefficient; $k$ is the number of studied and optimized factors in the experiment; $e$ is the random error.

### Experimental procedure

According to designed runs of the experiment through CCD, the adsorption of RR2 onto AC was carried out in a batch method as follows: 50 mL of dye solution with a concentration range of 100–500 mg $L^{-1}$, pH range of 3–11, adsorbent mass range of 0.25–12.25 g $L^{-1}$ was loaded into the flasks and maintained at the desired time in the range of 10–90 min at room temperature (25 ± 2 °C). Finally, the sample solution was immediately centrifuged (Shimi fan, Iran) and the spectrum of dye in the effluent solutions was recorded by UV-Vis spectrophotometer at 540 nm for RR2 dye. The equations based on mass balance were applied to calculate the quantity of dyes that were adsorbed in each unit mass of the adsorbent ($q_e$). The efficiency of the adsorption process and the equilibrium adsorption capacity (mg $g^{-1}$) were calculated using Equations (3) and (4), respectively.

$$\%\text{Removal} = \frac{C_0 - C_t}{C_0} \times 100 \tag{3}$$

$$q_e = (C_0 - C_e)\ \frac{V}{W} \tag{4}$$

where $C_0$ is the initial dye concentrations (mg $L^{-1}$); $C_e$ is the final dye concentrations (mg $L^{-1}$); $q_e$ is the amount of adsorbate per mass of the adsorbent (mg $g^{-1}$); $V$ is the volume of solution (L); $W$ is the mass of adsorbent (g).

## RESULT AND DISCUSSION

### Morphology of the prepared AC

Scanning electron microscopy (SEM) has been a primary tool for characterizing the surface morphology, size, crystallinity, and fundamental physical properties of the adsorbent (Iqbal *et al*. 2020). The SEM photograph shows rough and uneven layers on the surface of the active carbon made from grape wood (Figure 2). Also, the surface physical morphology of the AC shows a large pore in the form of the honeycomb structure. This surface property is an important factor that causes the dye to bind to the AC surface. It appears that dye molecules are coated on all the surfaces and pores of the AC after

**Table 2** | Independent variables and their levels for the design of the tests used in this study

| Parameter name | Unit | Symbols | Low | High |
|---|---|---|---|---|
| Contact time | min | $X_1$ | 10 | 90 |
| pH | – | $X_2$ | 3 | 11 |
| Adsorbent dosage | g | $X_3$ | 0.25 | 12.25 |
| Initial concentration | mg $L^{-1}$ | $X_4$ | 100 | 500 |

**Table 3** | Experimental design conditions for RR2 adsorption using AC

| Run | Time | pH | Dosage | Initial concentration | $C_1$ | R% |
|---|---|---|---|---|---|---|
| 1 | 90 | 3 | 0.25 | 100 | 71.33 | 28.66 |
| 2 | 10 | 11 | 0.25 | 100 | 88.66 | 11.33 |
| 3 | 10 | 3 | 0.25 | 100 | 85.66 | 14.33 |
| 4 | 90 | 11 | 0.25 | 100 | 77 | 23 |
| 5 | 90 | 11 | 12.25 | 100 | 4.66 | 95.33 |
| 6 | 90 | 3 | 12.25 | 100 | 2.33 | 97.66 |
| 7 | 10 | 11 | 12.25 | 100 | 62.66 | 37.33 |
| 8 | 10 | 3 | 12.25 | 100 | 58 | 42 |
| 9 | 50 | 7 | 6.25 | 200 | 39.33 | 80.33 |
| 10 | 50 | 9 | 6.25 | 300 | 134 | 55.33 |
| 11 | 30 | 7 | 6.25 | 300 | 158.33 | 47.1 |
| 12 | 50 | 5 | 6.25 | 300 | 110 | 63.4 |
| 13 | 50 | 7 | 6.25 | 300 | 125 | 58.3 |
| 14 | 50 | 7 | 6.25 | 300 | 127 | 57.6 |
| 15 | 50 | 7 | 6.25 | 300 | 121 | 59.6 |
| 16 | 50 | 7 | 3.25 | 300 | 175 | 41.6 |
| 17 | 50 | 7 | 3.25 | 300 | 177 | 41 |
| 18 | 50 | 7 | 3.25 | 300 | 174 | 42 |
| 19 | 50 | 7 | 9.25 | 300 | 95 | 68.33 |
| 20 | 50 | 7 | 6.25 | 300 | 124.33 | 58.5 |
| 21 | 70 | 7 | 6.25 | 300 | 107.66 | 64 |
| 22 | 50 | 7 | 6.25 | 400 | 140 | 65 |
| 23 | 10 | 11 | 0.25 | 500 | 500 | 0 |
| 24 | 10 | 3 | 0.25 | 500 | 500 | 0 |
| 25 | 90 | 3 | 12.25 | 500 | 207 | 58.6 |
| 26 | 90 | 11 | 0.25 | 500 | 500 | 0 |
| 27 | 10 | 11 | 12.25 | 500 | 451.66 | 9.66 |
| 28 | 10 | 3 | 12.25 | 500 | 438 | 12.4 |
| 29 | 90 | 11 | 12.25 | 500 | 221.66 | 55.66 |
| 30 | 90 | 3 | 0.25 | 500 | 500 | 0 |

adsorption. Therefore, the presence of a porous structure on the surface of AC increases RR2 adsorption on the surface of AC and as a result high RR2 removal.

FTIR is an analytical technique that with rotating and vibrating movements of the molecular groups and their chemical bonds causes adsorption in the infrared (IR) region to happen at 400–4,000 $cm^{-1}$ (Archin *et al.* 2019). Therefore, this method is used to identify functional groups in organic, polymeric, and inorganic materials (Iqbal *et al.* 2020). Figure 3 presents the FTIR spectrum of AC after adsorption that revealed different functional groups on the surface. The peaks of 1,000–800 $cm^{-1}$ are mainly due to the tensile vibration of Si–O. Also, the existence of different functional groups at 1,500 $cm^{-1}$ wavelengths is due to the stretching of the functional group (Ca–O). C=C aromatic stretching of lignin assigns the bands in the region 1,595 $cm^{-1}$. The appearance of a band at 1,322 $cm^{-1}$ can be attributed to C–O stretching vibrations in carboxylate groups. The spectrum at 1,994 $cm^{-1}$ due to the existence of the (C ≡ C) functional group and the wavelength of 3,200–3,600 $cm^{-1}$ related to the OH group from the hydroxyl functional group indicating the presence of functional groups present in the adsorbent (Mousavi *et al.* 2017; Archin *et al.* 2019). It is expected that the presence of different functional groups on the

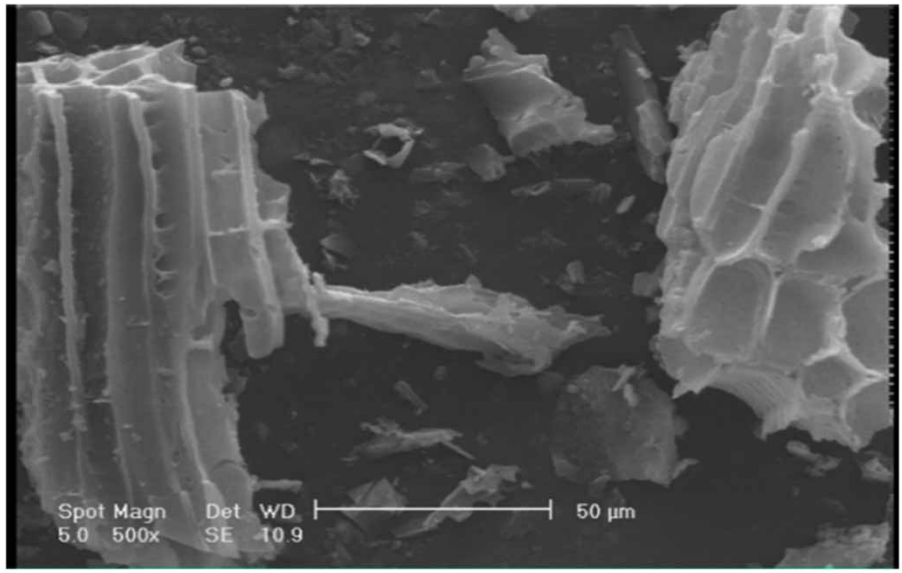


**Figure 2** | SEM of AC prepared from grape wood after adsorption.

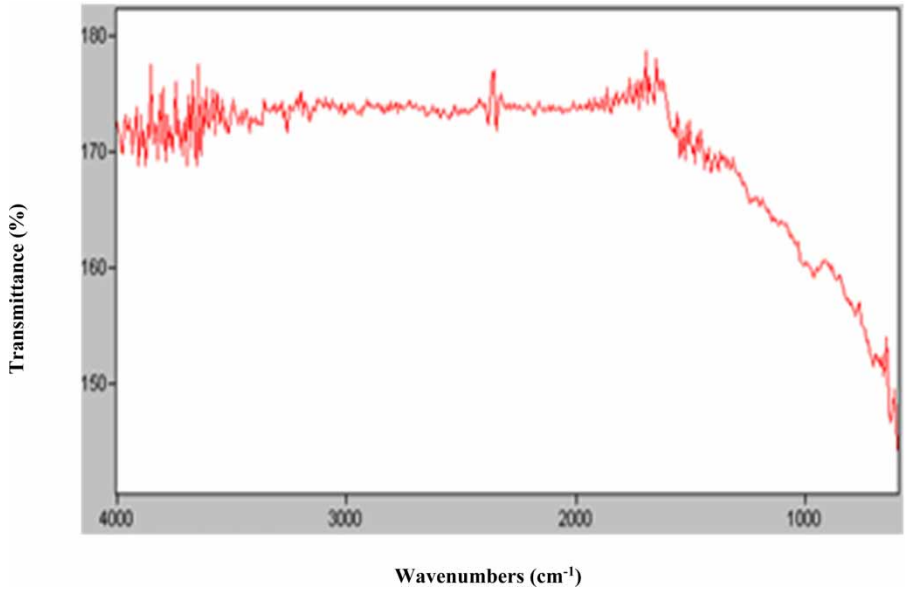


**Figure 3** | FTIR spectroscopy of produced carbon before adsorption.

surface of AC greatly helped the huge adsorption activities of RR2 dye in the wastewater. The fact that hydroxyl groups, carbonyl groups, ethers, and aromatic compounds are present reveals the lignocellulosic structure of grape wood.

### RSM approach and statistical analysis

In order to optimize the chosen adsorption factors, a CCD was applied. The design of experimental (DOE) software (version 8) was employed to investigate how pH, the amount of adsorbent, initial concentration, and the time of RR2 dye affect the responses. F-test was done in order to examine the statistical model and to find out the mathematical relationship between responses and process parameters including contact time (X1), pH (X2), adsorbent dosage (X3), and the initial concentration of RR2 (X4). The regression model was also examined for its significance and performance and it was done with the analysis of

variance ANOVA for the adsorption of RR2 dye using AC. The ANOVA results for the adsorption of RR2 dye are shown in Table 4. The *F*-value of the model (156.90) indicates that the model has a significant level. Only 0.01% of the '*F*-value of model' is likely to be due to noise. *P*-value is used to determine the significance of each parameter. The amounts of Prob > F when they are lower than 0.05 reveal that the model terms are acceptable for the adsorption of RR2 dye and that the parameters or their interactions are statistically significant. When they are more than 0.5 and are not significant, they reveal that the quadratic model is proper for this research. As shown in Table 4, the *P*-values of X1, X2, X3, X4, X1 × 3, and X3 × 4 are less than 0.05, indicating a significant effect of these variables on RR2 removal. Adsorbent dose and contact time have the greatest effect on RR2 adsorption. Pred $R^2$ and Adj $R^2$ for RR2 dye removal are 0.95 and 0.96, respectively, which confirms that there is a good match between predicted data and experimental data. The $R^2$ (Adj) and $R^2$ (pred) should be within approximately 0.2 of each other to be in reasonable agreement (Mousavi *et al.* 2017).

There is sufficient accuracy in comparing the range of the estimated amounts at the design points to the average estimation error. The coefficient of variation (CV) is a factor that expresses the standard deviation as the mean's percentage. Those amounts of CV that are lower, are more reproducible. Those amounts of CV that are lower are more reproducible. In the research, the amount of CV (CV% RR2: 12.92) was inside the approvable limit which was between 0.5 and 13.5%. The lack of fit value 416.33 is not significant and confirms that the model is adequate. Adequate precision measured the signal-to-noise ratio and a value of this parameter greater than 4 is generally essential.

## Effect of contact time and initial pH

The pH can affect the degree of ionization of the different pollutants, the surface charge of the adsorbent, the dissociation of functional groups on the active sites of the adsorbent as well as the structure of the dye molecule. So, pH plays an important

**Table 4** | The results from the ANOVA for the quadratic equation

| Source | Sum of squares | *df* | Mean square | *F*-value | *P*-value |
|---|---|---|---|---|---|
| Model | 65,602.65 | 14 | 4,685.90 | 156.90 | <0.0001 |
| $X_1$ | 10,783.36 | 1 | 10,783.36 | 361.06 | <0.0001 |
| $X_2$ | 382.50 | 1 | 382.50 | 12.81 | 0.0007 |
| $X_3$ | 22,408.69 | 1 | 22,408.69 | 750.32 | <0.0001 |
| $X_4$ | 7,477.79 | 1 | 7,477.79 | 250.38 | <0.0001 |
| $X_1$ $X_2$ | 27.45 | 1 | 27.45 | 0.92 | 0.3414 |
| $X_1$ $X_3$ | 7,161.41 | 1 | 7,161.41 | 239.79 | <0.0001 |
| $X_1$ $X_4$ | 113.78 | 1 | 113.78 | 3.81 | 0.0554 |
| $X_2X_3$ | 16.69 | 1 | 16.69 | 0.56 | 0.4576 |
| $X_2$ $X_4$ | 2.57 | 1 | 2.57 | 0.086 | 0.7704 |
| $X_3$ $X_4$ | 458.19 | 1 | 458.19 | 15.34 | 0.0002 |
| $x_1^2$ | 361.09 | 1 | 361.09 | 12.09 | 0.0009 |
| $x_2^2$ | 361.09 | 1 | 149.34 | 5.00 | 0.0289 |
| $x_3^2$ | 382.89 | 1 | 382.89 | 12.82 | 0.0007 |
| $x_4^2$ | 854.06 | 1 | 854.06 | 28.60 | <0.0001 |
| Residual | 1,881.53 | 63 | 29.87 | | |
| Lack of fit | 416.33 | 10 | 41.63 | 1.51 | 0.1633 |
| Pure error | 1,465.21 | 53 | 27.65 | | |
| Cor. total | 67,484.18 | 77 | | | |
| Std. dev. | 5.46 | | | | |
| Mean | 42.29 | | | | |
| C.V.% | 12.92 | | | | |
| Adeq Precision | 42.651 | | | | |

role in the adsorption capacity of the dye by affecting the chemistry of the dye molecule and the AC prepared in the aqueous solution (Purkait *et al*. 2005; Bazrafshan *et al*. 2013). Figure 4 shows the effect of initial pH on RR2 dye adsorption onto AC obtained from grape wood wastes. The adsorption of RR2 dye onto AC obtained from grape wood wastes is highly dependent on solution pH. The adsorption capacity of RR2 dye decreases with increasing solution pH from 3 to 11. The maximum RR2 removal efficiency was achieved at about 97.96% at pH of 3. Given that at lower pH, there is a high electrostatic attraction between the protons of the $-NH_2$ and $-SO_3H$ groups in the RR2 dye structure, but at higher pH, electrostatic repulsion forces are increased between the ionized groups and as a result, the dye adsorption is reduced (Dash *et al*. 2016). Georgin *et al*. (2016) used peanut shells to make AC as a new low-cost adsorbent to remove Reactive Red 141 (RR141) from aqueous solutions. The results of this study show that the maximum absorption of RR141 is at acidic pH (pH: 2.5) (Georgin *et al*. 2016). A similar trend was found by Mahanna and Samy in the adsorption of Reactive Red 195 (RR195) dye onto soybean leaves. The solution pH strongly affects RR195 removal efficiency. The highest removal efficiency equal to 97.8% was achieved using a solution pH equal to 1 at 50 °C (Mahanna & Azab 2020).

One of the important and effective factors in the adsorption process is the duration time of interaction between the adsorbent surface and the contaminant (e.g. RR2 dye), which has an effective role in the kinetics and speed of the adsorption process (Foroutan *et al*. 2021). The contact time between adsorbent and adsorbent material is significantly affected the dye removal efficiency (Mousavi *et al*. 2021). It is essential to evaluate the effect of contact time required to reach equilibrium for designing batch adsorption experiments. Therefore, the effect of contact time on the adsorption of RR2 dye was investigated. The data indicate that the adsorption capacity and percentage removal of RR2 dye go on increasing with the increase of contact time and the maximum value of RR2 adsorption is about 97.96% after 90 min. Figure 4 shows that the rate of adsorption of RR2 is fast initially and then becomes slower and dye adsorption equilibrium has been attained. As initially, the whole of the surface is free for adsorption. But with an increase of contact time, more and more RR2 dye particles get adsorbed over the surface and the free surface for adsorption decreases hence the rate of adsorption also decreases. In fact, the mechanism of RR2 dye removal by the adsorbent includes (1) migration of the RR2 dye from the bulk of the solution to the surface of the adsorbent, (2) diffusion of the RR2 dye through the boundary layer to the surface of the adsorbent, (3) intraparticle diffusion of the RR2 dye in the internal pores of the adsorbent particle. In addition, the rate of adsorption and the increase in contact

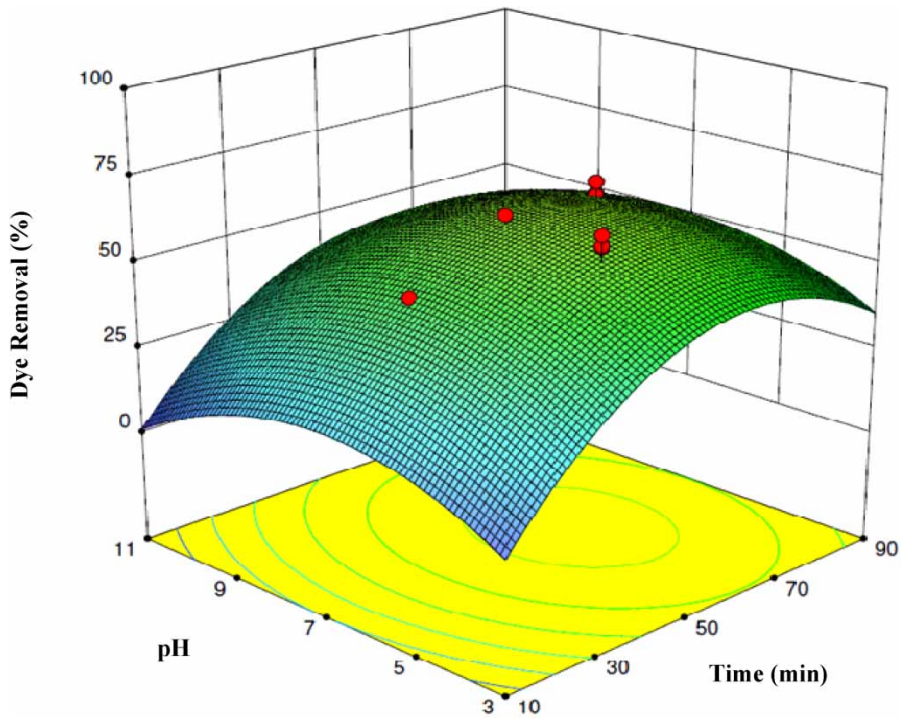


**Figure 4** | Three-dimensional (3D) response surface plot showing the effect of contact time and pH on RR2 removal at fixed (adsorbent dosage 6.25 g $L^{-1}$ and initial concentration 300 mg $L^{-1}$).

time can affect the resistance of the boundary layer (Kaur & Kaur 2014). These results were in agreement with the study carried out by Almasi *et al.* (2017) which used walnut shells to prepare AC; they found that the contact time has significant effects on the removal of RR2 dye (Almasi *et al.* 2017).

### Effect of dye concentration and adsorbent dosage

The initial dye concentration plays an important role in determining the driving force between the surface of the adsorbent and the dye solution bulk. In fact, the presence of large amounts of dye concentration at a constant adsorbent dosage in the solution has two opposing belongings; it increases the quantity of adsorbed dye and decreases the equilibrium time, however it decreases the removal efficiency (Abdel-Aziz *et al.* 2021). The effect of initial dye concentration and adsorbent dosage on the removal of RR2 is shown in Figure 5. From the figure, it was evident that the removal of dye increased with decreasing dye concentration. When the initial concentration of the RR2 is the lowest amount (100 mg $L^{-1}$), the value of removal efficiency is 97.96%. So that when the dye concentration increased from 100 to 500 mg $L^{-1}$, the dye removal efficiency decreased from 97.96% to 58.6%. In fact, in low concentrations of dye, the percentage of the adsorbent-free surface to the number of dye fragments is high. Therefore, dye adsorption becomes easier and faster. While at high concentrations of dye, the percentage of the adsorbent-free surface decreases the number of dye fragments. Also, rapid saturation of the adsorbent at high concentrations of the dye can damage the surface locations of the adsorbent (Etim *et al.* 2016).

One of the important and influencing parameters on absorption performance is the adsorbent dose. The influence of adsorbent dose in the adsorption of RR2 dye was studied to obtain the most appropriate amount of adsorbent at various RR2 dye concentrations (Kuang *et al.* 2020). In order to determine the effect of adsorbent dosage on the adsorption process, 0.25–12.25 g $L^{-1}$ adsorbent was used for adsorption experiments. From Figure 5, it was evident that the removal of RR2 dye increased with increasing adsorbent dose. In fact, with increasing the adsorbent dose, the access of dye to the adsorbent surface and active sites on the adsorbent surface increases (Abechi *et al.* 2011). This trend continues until all the dye molecules absorb on the adsorbent active sites (Sartape *et al.* 2017). A similar trend was found by Mousavi *et al.* (2021) in the adsorption

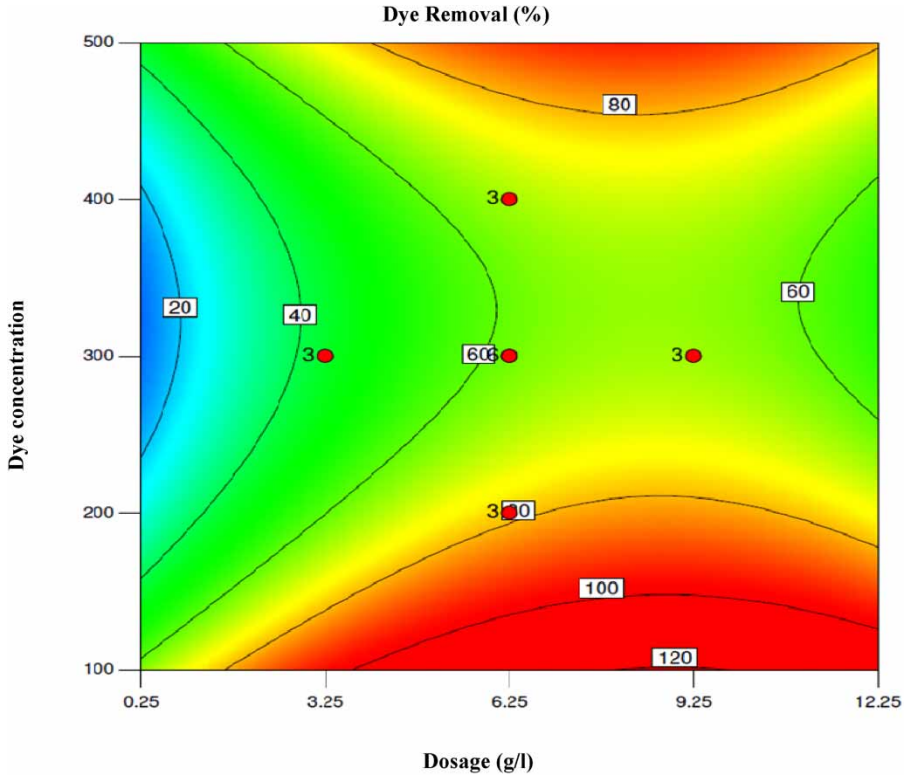


**Figure 5** | Two-dimensional response surface plot showing the effect of dye concentration and adsorbent dosage on RR2 removal at fixed (pH: 7 and contact time: 90 min).

of RR2 dye onto grape wood waste. In this study, the activating chemical substance sulfuric acid was used for the chemical preparation of AC. According to the results of this study, the highest adsorption rate was obtained in 12.25 g $L^{-1}$ of AC which was 96.83% (Mousavi *et al.* 2021). Therefore, it can be concluded that the use of phosphoric acid as an activating agent leads to the improvement of the performance of AC in the removal of dye.

### Equilibrium isotherms

Adsorption isotherms describe the relationship between the amount of adsorbed dye on the adsorbent and the final dye concentration in the solution. Experimental results have been analyzed using three two-parameter isotherm models including Freundlich, Langmuir, and Tempkin (Tosun 2012).

### Langmuir adsorption isotherm

The Langmuir isotherm describes the formation of a monolayer adsorbent on the outer surface of the adsorbent, and after that no further adsorption takes place. The Langmuir isotherm is valid for monolayer adsorption onto a surface containing a finite number of identical sites. The model assumes uniform energies of adsorption onto the surface and no transmigration of adsorbate in the plane of the surface (Nekouei *et al.* 2015). The linear form of this model is as follows (Equation (5)) (Hettithanthri *et al.* 2022):

$$\frac{C_e}{q_e} = \frac{C_e}{Q_m} + \frac{1}{KQ_m} \tag{5}$$

where $C_e$ is the equilibrium concentration of adsorbate (mg $L^{-1}$); $q_e$ is the amount of dye adsorbed per gram of the adsorbent at equilibrium (mg $g^{-1}$); $Q_m$ is the maximum monolayer coverage capacity (mg $g^{-1}$); $K_L$ is the Langmuir isotherm constant (Lm $g^{-1}$).

The Langmuir plot ($C_e/q_e$ vs. $C_e$) for RR2 adsorption at room temperatures gives a straight line and the value of $Q_m$ and $K_L$ constants and the correlation coefficients for this model are presented in Table 5 and Figure 6. The isotherm of RR2 on AC was found to be linear over the whole concentration range studies with extremely high correlation coefficients ($R^2$:0.91). The essential features of the Langmuir isotherm may be expressed in terms of the equilibrium parameter RL, which is a dimensionless constant referred to as the separation factor or equilibrium parameter (Equation (6)):

$$RL = \frac{1}{1 + KLC_0} \tag{6}$$

where: $C_0$ is the initial concentration; $K_L$ is the constant related to the energy of adsorption (Langmuir Constant).

RL value indicates the adsorption nature to be either unfavorable if RL > 1, linear if RL = 1, favorable if 0 < RL < 1, and irreversible if RL = 0. From the data calculated in Table 3, the RL is greater than 0 but less than 1 indicating that Langmuir isotherm is favorable (Selvam *et al.* 2021).

### Freundlich adsorption isotherm

The adsorption data obtained was also analyzed with the Freundlich isotherm model. Another well-known model is the Freundlich isotherm which, unlike the Langmuir model, expresses dye adsorption on heterogeneous surfaces. The linear pattern is as follows (Equation (7)):

$$\ln q_e = \ln K_f + \frac{1}{n} \ln C_e \tag{7}$$

**Table 5** | Isotherm model parameters and correlation coefficients for RR2 adsorption on AC

| Isotherm | Langmuir | | | Freundlich | | | Temkin | |
|---|---|---|---|---|---|---|---|---|
| Parameter | $R^2$ | $q_m$ | $K_1$ | $R^2$ | $K_f$ | 1/n | $R^2$ | B |
| Value | 0.91 | 33 | 0.0007 | 0.96 | 8.51 | 0.66 | 0.99 | 0.37 |

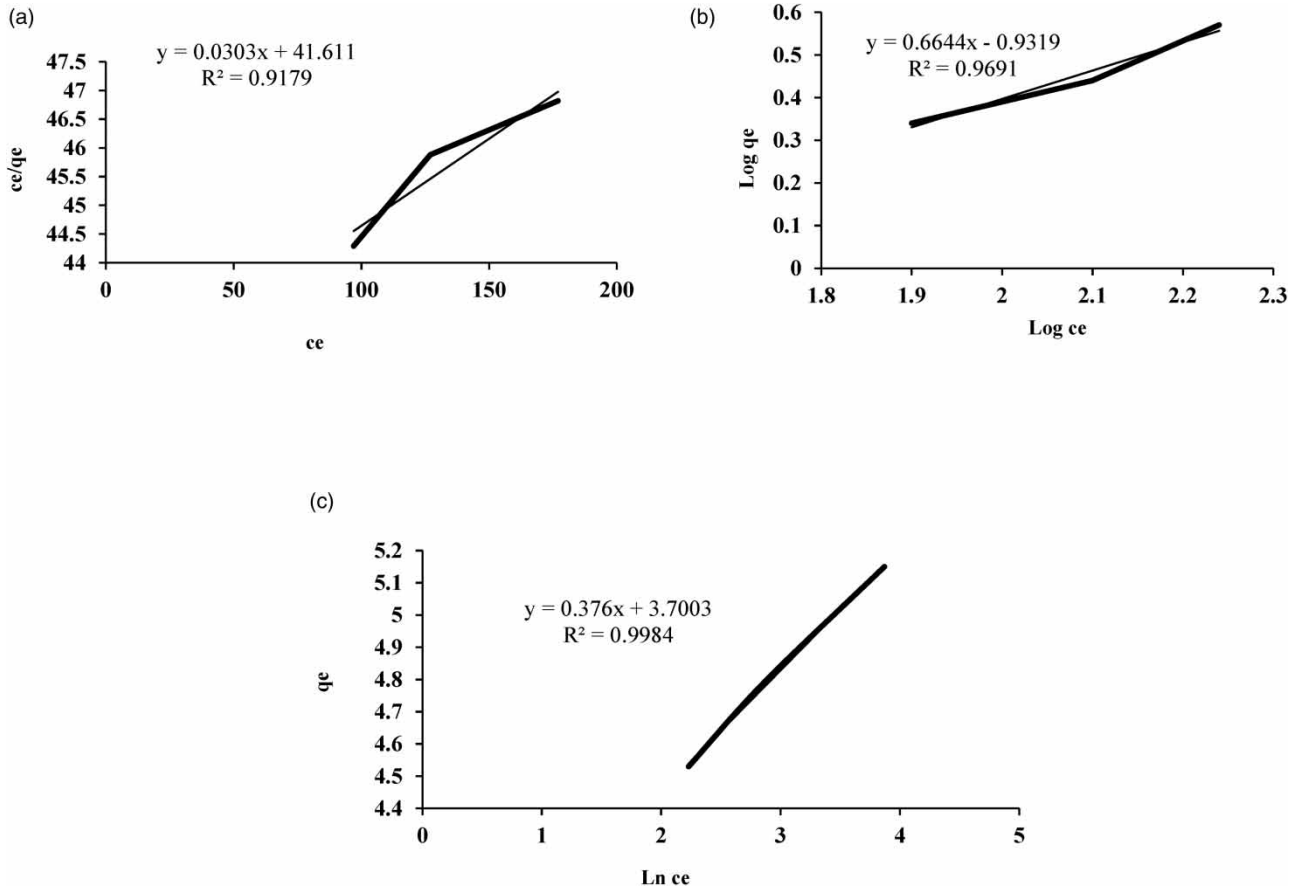


**Figure 6** | Isotherm plots (a) Langmuir, (b) Freundlich, and (c) Temkin for RR2 adsorption onto prepared adsorbent (pH 7, adsorbent dosage of 6.25 g $L^{-1}$ at 25 °C).

where $K_f$ is the Freundlich isotherm constant (mg $g^{-1}$); $n$ is the adsorption intensity; $C_e$ is the equilibrium concentration of adsorbate (mg $L^{-1}$); $q_e$ is the amount of dye adsorbed per gram of the adsorbent at equilibrium (mg $g^{-1}$).

The Freundlich isotherm constants $K_f$ and $1/n$ can be reported based on the plot of $\ln q_e$ versus $\ln C_e$, which has been presented in Figure 6. In the adsorption process, the magnitude of the exponent, 1/n indicates the favorability of adsorption. If the values are $1/n < 1$, it indicates that with the appearance of new adsorption sites, the type of isotherm to be required, the adsorption intensity, and the adsorption capacity increase. On the other hand, if it is $1/n > 1$, it indicates the adsorption bond weakens, which reduces the dye adsorption capacity (Gholamiyan *et al.* 2020).

### Tempkin adsorption isotherm

This isotherm contains a factor that explicitly takes into the account of adsorbent–adsorbate interactions. By ignoring the extremely low and large value of concentrations, the model assumes that heat of adsorption (function of temperature) of all molecules in the layer would decrease linearly rather than logarithmic with coverage. As implied in the equation, its derivation is characterized by a uniform distribution of binding energies (up to some maximum binding energy) was carried out by plotting the quantity adsorbed $q_e$ against $\ln C_e$ and the constants were determined from the slope and intercept (Allen *et al.* 2004; Dada *et al.* 2012). The model is given by the following Equation (8) (Santhi *et al.* 2010):

$$q_e = B\ Ln\ k_t + B\ Ln\ C_e$$
$$B = \frac{RT}{b_T} \tag{8}$$

where $k_t$ represents Temkin isotherm equilibrium binding constant (L g$^{-1}$); $b_T$ is the Temkin isotherm constant; $R$ is the universal gas constant (8.314 J/mol/K); $T$ is the temperature in Kelvin; $B$ is the constant related to heat of adsorption (J mol$^{-1}$).

### Kinetic study

Several kinetic models are used to examine the controlling mechanism of the adsorption process such as chemical reaction and diffusion control. The kinetics of adsorption of RR2 dye on AC are described by using first-order and pseudo-second-order model (Figure 7 and Table 6).

### The pseudo-first-order model

The pseudo-first-order rate expression based on solid capacity is generally expressed as follows (Equation (9)) (Akar *et al.* 2016):

$$\log (q_e - q_t) = \log q_e - \frac{kl}{2.303} t \tag{9}$$

### The pseudo-second-order model

The pseudo-second-order equation is also based on the sorption capacity of the solid phase. It predicts the behavior over the whole range of data. Furthermore, it is in agreement with chemisorption being the rate controlling step and is expressed as (Equation (10)) (Abdel Wahab 2007; Inyinbor *et al.* 2017):

$$\frac{t}{q_t} = \frac{1}{k_2\ q_e^2} + \frac{1}{q_e} t \tag{10}$$

where $q_e$ is the amount of dye adsorbed at equilibrium (mg g$^{-1}$); $q_t$ is the amount of dye adsorbed at any time t (mg g$^{-1}$); $K_1$ is the first-order rate constant (min$^{-1}$); $K_2$ is the pseudo-second-order rate constant (g mg$^{-1}$ min$^{-1}$).

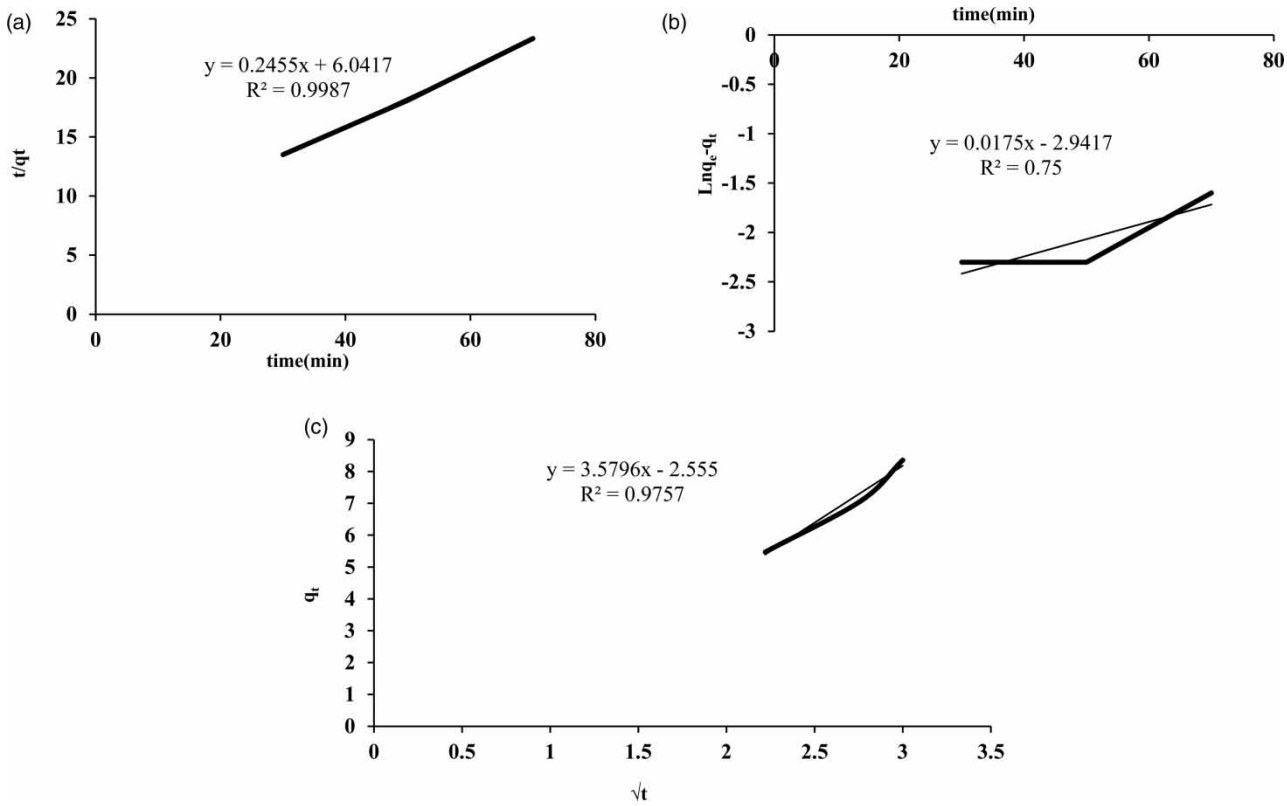


**Figure 7** | (a) Pseudo-second-order, (b) pseudo-first-order, and (c) intraparticle diffusion kinetic plots for the adsorption of RR2 onto prepared adsorbent (pH 7, adsorbent dosage of 6.25 g L$^{-1}$ at 25 °C).

**Table 6** | Comparison of pseudo-first-order, pseudo-second-order, and intraparticle diffusion adsorption rate constants

| Kinetic models | | | | | | | |
|---|---|---|---|---|---|---|---|
| Pseudo-first-order | | | Pseudo-second-order | | | Intraparticle diffusion | |
| $K_1$ | $q_e$ | $R^2$ | $K_2$ | $q_e$ | $R^2$ | $K_{id}$ | $R^2$ |
| 0.04 | 870.96 | 0.75 | 0.009 | 4.08 | 0.99 | 354.88 | 0.97 |

### Intraparticle diffusion model

Intraparticle diffusion, followed by a plateau to equilibrium where the intraparticle diffusion starts to decrease due to the low concentration in solution as well as fewer available adsorption sites (Ong *et al.* 2007). Intraparticle diffusion was characterized using the relationship between specific sorption ($q_t$) and the square root of time ($t^{1/2}$) as shown below (Equation (11)) (Inyinbor *et al.* 2017):

$$q_t = Kd\ \sqrt{t} + c \tag{11}$$

where $q_t$ is the amount of RR2 absorbed at time t (mg $g^{-1}$); $Kd$ is the rate of diffusion within the particles (mg/(g $min^{0.5}$); $C$ represents the thickness of the boundary (mg $g^{-1}$).

## CONCLUSION

An AC was prepared from grape wood waste and used for the removal of RR2 from aqueous solutions. The AC was prepared using a chemical activation method with phosphoric acid as the activating agent. The prepared AC was characterized using different types of analytical techniques such as SEM and FTIR analysis. Batch adsorption tests demonstrate that the adsorption is affected by various conditions, such as initial pH, adsorbent dosage, contact time, and initial dye concentration. From the present study, it can be seen that the AC obtained from grape wood wastes can be used effectively for the removal of the RR2 dye from aqueous solutions. Using the Design-Expert software, the optimum parameter conditions of 100 mg $L^{-1}$ of initial RR2 concentration, 90 min of contact time, 12.25 g $L^{-1}$ of adsorbent dose, and pH of 3 were determined. This adsorbent was able to remove up to 97.96% of RR2 dye from solutions whose initial concentration varied between 100 and 500 mg $L^{-1}$. The experimental data follow the Temkin isotherm and pseudo-second-order models. Finally, the results support the ability of grape wood to be a promising precursor for production of highly porous AC suitable for the removal of azo dyes (e.g. RR2). Overall, these experimental and theoretical results provided new insights into the RR2 dye adsorption mechanism.

## ACKNOWLEDGEMENTS

The authors gratefully acknowledge the Research Council of Kermanshah University of Medical Sciences for the financial support through grant number 50002046.

## DECLARATION OF COMPETING INTEREST

The authors declare that they have no known competing financial interests or personal relationships that could have appeared to influence the work reported in this paper.

## DATA AVAILABILITY STATEMENT

All relevant data are included in the paper or its Supplementary Information.

## CONFLICT OF INTEREST

The authors declare there is no conflict.

## REFERENCES

Abdel-aziz, M. H., El-ashtoukhy, E. Z., Bassyouni, M., Al-hossainy, A. F., Fawzy, E. M., Abdel-hamid, S. & Zoromba, M. S. 2021 DFT and experimental study on adsorption of dyes on activated carbon prepared from apple leaves. *Carbon Letters* **31**, 863–878.

Abdel Wahab, O. 2007 Kinetic and isotherm studies of copper (II) removal from wastewater using various adsorbents. *Egyptian Journal of Aquatic Research* **33** (1), 125–143.

Abechi, E., Gimba, C., Uzairu, A. & Kagbu, J. 2011 Kinetics of adsorption of methylene blue onto activated carbon prepared from palm kernel shell. *Archives of Applied Science Research* **3**, 154–164.

Akar, S. T., San, E. & Akar, T. 2016 Chitosan–alunite composite: an effective dye remover with high sorption, regeneration and application potential. *Carbohydrate Polymers* **143**, 318–326.

Ali, A. F., Kovo, A. S. & Adetunji, S. A. 2017 Methylene blue and brilliant green dyes removal from aqueous solution using agricultural wastes activated carbon. *Journal of Encapsulation and Adsorption Sciences* **7**, 95–107.

Allen, S., Mckay, G. & Porter, J. F. 2004 Adsorption isotherm models for basic dye adsorption by peat in single and binary component systems. *Journal of Colloid and Interface Science* **280** (2), 322–333.

Almasi, A., Rostamkhani, Z. & Mousavi, S. A. 2017 Adsorption of reactive Red 2 using activated carbon prepared from walnut shell: batch and fixed bed studies. *Desalination and Water Treatment* **79**, 356–367.

Archin, S., Sharifi, S. H. & Asadpour, G. 2019 Optimization and modeling of simultaneous ultrasound-assisted adsorption of binary dyes using activated carbon from tobacco residues: response surface methodology. *Journal of Cleaner Production* **239**, 118136.

Bazrafshan, E., Ahmadabadi, M. & Mahvi, A. H. 2013 Reactive Red-120 removal by activated carbon obtained from cumin herb wastes. *Fresenius Environmental Bulletin* **22**, 584–590.

Cherifi, H., Fatiha, B. & Salah, H. 2013 Kinetic studies on the adsorption of methylene blue onto vegetal fiber activated carbons. *Applied Surface Science* **282**, 52–59.

Dada, A., Olalekan, A., Olatunya, A. & Dada, O. 2012 Langmuir, Freundlich, Temkin and Dubinin–Radushkevich isotherms studies of equilibrium sorption of $Zn^{2+}$ unto phosphoric acid modified rice husk. *IOSR Journal of Applied Chemistry* **3**, 38–45.

Dash, S., Chaudhuri, H., Udayabhanu, G. & Sarkar, A. 2016 Fabrication of inexpensive polyethylenimine-functionalized fly ash for highly enhanced adsorption of both cationic and anionic toxic dyes from water. *Energy & Fuels* **30** (8), 6646–6653.

Demiral, İ., Samdan, C. & Demiral, H. 2021 Enrichment of the surface functional groups of activated carbon by modification method. *Surfaces and Interfaces* **22**, 100873.

Etim, U., Umoren, S. & Eduok, U. 2016 Coconut coir dust as a low cost adsorbent for the removal of cationic dye from aqueous solution. *Journal of Saudi Chemical Society* **20**, S67–S76.

Foroutan, R., Peighambardoust, S. J., Peighambardoust, S. H., Pateiro, M. & Lorenzo, J. M. 2021 Adsorption of crystal violet dye using activated carbon of lemon wood and activated carbon/$Fe_3O_4$ magnetic nanocomposite from aqueous solutions: a kinetic, equilibrium and thermodynamic study. *Molecules* **26** (8), 2241.

Gao, Y., Yue, Q., Gao, B. & Li, A. 2020 Insight into activated carbon from different kinds of chemical activating agents: a review. *Science of the Total Environment* **746**, 141094.

Georgin, J., Dotto, G. L., Mazutti, M. A. & Foletto, E. L. 2016 Preparation of activated carbon from peanut shell by conventional pyrolysis and microwave irradiation-pyrolysis to remove organic dyes from aqueous solutions. *Journal of Environmental Chemical Engineering* **4** (1), 266–275.

Ghaedi, A. M., Karamipour, S., Vafaei, A., Baneshi, M. M. & Kiarostami, V. 2019 Optimization and modeling of simultaneous ultrasound-assisted adsorption of ternary dyes using copper oxide nanoparticles immobilized on activated carbon using response surface methodology and artificial neural network. *Ultrasonics Sonochemistry* **51**, 264–280.

Gholamiyan, S., Hamzehloo, M. & Farrokhnia, A. 2020 RSM optimized adsorptive removal of erythromycin using magnetic activated carbon: adsorption isotherm, kinetic modeling and thermodynamic studies. *Sustainable Chemistry and Pharmacy* **17**, 100309.

González-García, P. 2018 Activated carbon from lignocellulosics precursors: a review of the synthesis methods, characterization techniques and applications. *Renewable and Sustainable Energy Reviews* **82**, 1393–1414.

Hameed, B. B. & Ismail, Z. Z. 2018 Decolorization, biodegradation and detoxification of reactive red azo dye using non-adapted immobilized mixed cells. *Biochemical Engineering Journal* **137**, 71–77.

Heidarinejad, Z., Dehghani, M. H., Heidari, M., Javedan, G., Ali, I. & Sillanpää, M. 2020 Methods for preparation and activation of activated carbon: a review. *Environmental Chemistry Letters* **18**, 393–415.

Hettithanthri, O., Rajapaksha, A. U., Keerthanan, S., Ramanayaka, S. & Vithanage, M. 2022 Colloidal biochar for enhanced adsorption of antibiotic ciprofloxacin in aqueous and synthetic hydrolyzed human urine matrices. *Chemosphere* **297**, 133984.

Inyinbor, A., Adekola, F. & Olatunji, G. 2017 Liquid phase adsorptions of rhodamine B dye onto raw and chitosan supported mesoporous adsorbents: isotherms and kinetics studies. *Applied Water Science* **7**, 2297–2307.

Iqbal, D. N., Tariq, M., Khan, S. M., Gull, N., Iqbal, S. S., Aziz, A., Nazir, A. & Iqbal, M. 2020 Synthesis and characterization of chitosan and guar gum based ternary blends with polyvinyl alcohol. *International Journal of Biological Macromolecules* **143**, 546–554.

Jensen, W. A. 2017 Response surface methodology: process and product optimization using designed experiments. *Journal of Quality Technology* **49**, 186.

Jha, M. K., Joshi, S., Sharma, R. K., Kim, A. A., Pant, B., Park, M. & Pant, H. R. 2021 Surface modified activated carbons: sustainable bio-based materials for environmental remediation. *Nanomaterials* **11** (11), 3140.

Jjagwe, J., Olupot, P. W., Menya, E. & Kalibbala, H. M. 2021 Synthesis and application of granular activated carbon from biomass waste materials for water treatment: a review. *Journal of Bioresources and Bioproducts* **6** (4), 292–322.

Karimifard, S. & Moghaddam, M. R. A. 2018 Application of response surface methodology in physicochemical removal of dyes from wastewater: a critical review. *Science of the Total Environment* **640**, 772–797.

Kaur, H. & Kaur, R. 2014 Removal of Rhodamine-B dye from aqueous solution onto Pigeon Dropping: adsorption, kinetic, equilibrium and thermodynamic studies. *Journal of Materials and Environmental Science* **5**, 1830–1838.

Kuang, Y., Zhang, X. & Zhou, S. 2020 Adsorption of methylene blue in water onto activated carbon by surfactant modification. *Water* **12** (2), 587.

Lopes, R. P. & Astruc, D. 2021 Biochar as a support for nanocatalysts and other reagents: recent advances and applications. *Coordination Chemistry Reviews* **426**, 213585.

Lotfy, H. R. & Roubík, H. 2021 Water purification using activated carbon prepared from agriculture waste – overview of a recent development. *Biomass Conversion and Biorefinery* 1–14.

Maas, R. & Chaudhari, S. 2005 Adsorption and biological decolourization of azo dye reactive Red 2 in semicontinuous anaerobic reactors. *Process Biochemistry* **40** (2), 699–705.

Mahanna, H. & Azab, M. 2020 Adsorption of reactive Red 195 dye from industrial wastewater by dried soybean leaves modified with acetic acid. *Desalination and Water Treatment* **178**, 312–321.

Mendonça, A. R. V., Zanardi, G. B., Brum, S. S., Decampos, T. A., Cardoso, C. M. M. & Zavarize, D. G. 2019 RR2 dye adsorption to Hymenaea courbaril L. bark activated carbon associated with biofilm. *Environmental Science and Pollution Research* **26**, 28524–28532.

Mousavi, S., Mehralian, M., Khashij, M. & Parvaneh, S. 2017 Methylene Blue removal from aqueous solutions by activated carbon prepared from N. microphyllum (AC-NM): RSM analysis, isotherms and kinetic studies. *Global Nest Journal* **19** (4), 697–705.

Mousavi, S. A., Shahbazi, D., Mahmoudi, A., Mohammadi, P. & Massahi, T. 2021 Statistical modeling and kinetic studies on the adsorption of reactive Red 2 by a low-cost adsorbent: grape waste-based activated carbon using sulfuric acid activator-assisted thermal activation. *Adsorption Science & Technology* **2021**, 13.

Nekouei, F., Nekouei, S., Tyagi, I. & Gupta, V. K. 2015 Kinetic, thermodynamic and isotherm studies for acid blue 129 removal from liquids using copper oxide nanoparticle-modified activated carbon as a novel adsorbent. *Journal of Molecular Liquids* **201**, 124–133.

Nguyen, V. T., Nguyen, T. B., Dat, N. D., Huu, B. T., Nguyen, X. C., Tran, T., Bui, M. H., Dong, C. D. & Bui, X. T. 2022 Adsorption of norfloxacin from aqueous solution on biochar derived from spent coffee ground: master variables and response surface method optimized adsorption process. *Chemosphere* **288**, 132577.

Ong, S. A., Seng, C. E. & Lim, P. 2007 Kinetics of adsorption of Cu (II) and Cd (II) from aqueous solution on rice husk and modified rice husk. *Electronic Journal of Environmental, Agricultural and Food Chemistry* **6** (1573–4377), 1764–1774.

Onu, C. E., Nwabanne, J. T., Ohale, P. E. & Asadu, C. O. 2021 Comparative analysis of RSM, ANN and ANFIS and the mechanistic modeling in eriochrome black-T dye adsorption using modified clay. *South African Journal of Chemical Engineering* **36**, 24–42.

Paraskeva, P., Kalderis, D. & Diamadopoulos, E. 2008 Production of activated carbon from agricultural by-products. *Journal of Chemical Technology & Biotechnology: International Research in Process, Environmental & Clean Technology* **83** (5), 581–592.

Purkait, M., Dasgupta, S. & De, S. 2005 Adsorption of eosin dye on activated carbon and its surfactant based desorption. *Journal of Environmental Management* **76** (2), 135–142.

Santhi, T., Manonmani, S. & Smitha, T. 2010 Kinetics and isotherm studies on cationic dyes adsorption onto annona squmosa seed activated carbon. *International Journal of Engineering Science and Technology* **2** (3), 287–295.

Sartape, A. S., Mandhare, A. M., Jadhav, V. V., Raut, P. D., Anuse, M. A. & Kolekar, S. S. 2017 Removal of malachite green dye from aqueous solution with adsorption technique using Limonia acidissima (wood apple) shell as low cost adsorbent. *Arabian Journal of Chemistry* **10**, S3229–S3238.

Selvam, K., Sudhakar, C. & Selvankumar, T. 2021 Activated carbon derived from Borassus flabellifer fruit husk waste for enhanced removal of reactive red 120. *Environmental Technology & Innovation* **23**, 101752.

Selvanathan, N., Subki, N. S. & Sulaiman, M. A. 2015 Dye adsorbent by activated carbon. *Journal Of Tropical Resources and Sustainable Science* **3**, 169–173.

Shahbazi, D., Mousavi, S. & Nayeri, D. 2020 Low-cost activated carbon: characterization, decolorization, modeling, optimization and kinetics. *International Journal of Environmental Science and Technology* **17**, 3935–3946.

Tosun, İ. 2012 Ammonium removal from aqueous solutions by clinoptilolite: determination of isotherm and thermodynamic parameters and comparison of kinetics by the double exponential model and conventional kinetic models. *International Journal of Environmental Research and Public Health* **9** (3), 970–984.

Ukanwa, K. S., Patchigolla, K., Sakrabani, R., Anthony, E. & Mandavgane, S. 2019 A review of chemicals to produce activated carbon from agricultural waste biomass. *Sustainability* **11** (22), 6204.

Vishani, D. B. & Shrivastav, A. 2022 Chapter 19. Enzymatic decolorization and degradation of azo dyes. In: M. P. Shah, S. Rodriguez-Couto & R. Thapar Kapoor, eds. *Development in Wastewater Treatment Research and Processes, Innovative Microbe-Based Applications for Removal of Chemicals and Metals in Wastewater Treatment Plants.* Elsevier, Amsterdam, pp. 419–432.

Wong, S., Ngadi, N., Inuwa, I. M. & Hassan, O. 2018 Recent advances in applications of activated carbon from biowaste for wastewater treatment: a short review. *Journal of Cleaner Production* **175**, 361–375.

First received 17 July 2022; accepted in revised form 16 November 2022. Available online 15 December 2022